Geoderma 305 (2017) 293–304

Contents lists available at ScienceDirect

Geoderma

journal homepage: www.elsevier.com/locate/geoderma

Human health risk assessment and source analysis of metals in soils along the G324 Roadside, China, by Pb and Sr isotopic tracing

Jingwei Sun[a,b], Gongren Hu[a,c,*], Ruilian Yu[a], Chengqi Lin[a], Xiaoming Wang[d], Yaoyi Huang[b]

[a] College of Chemical Engineering, Huaqiao University, Xiamen 361021, China
[b] School of Resources and Environmental Science, Quanzhou Normal University, Quanzhou 362000, China
[c] State Key Laboratory of Environmental Geochemistry, Institute of Geochemistry, Chinese Academy of Sciences, Guiyang 550002, china
[d] Analytical Laboratory of Beijing Research Institute of Uranium Geology, Beijing 100029, China

ARTICLE INFO

Keywords:
G324 roadside
Metals
Multivariate statistical analysis
Pb and Sr isotope tracing
Potential ecological risk index
Human health risk

ABSTRACT

Metal pollution was studied along the G324 roadside in Xiamen, southeast China, based on the soil profile and the different distances from the road. A range of metal concentrations were determined using ICP-MS and evaluated using enrichment factors, human health risk assessment and potential ecological risk index. The pollution sources in the soil were examined using multivariate statistical analysis and Pb-Sr isotope tracing technology. The results showed that the high soil metal contents were mainly distributed at the depth of 0-30 m, and the distance from the highway of 0-7 m. In both topsoils and profile soils, Cd had the biggest ecological risk. According to the human health risk assessment, there is no risk for human health in the roadside. The multivariate statistical analysis showed that the surface soil was clearly affected by the traffic factors; however, the profile soil was not only influenced by the traffic factors, but also by the industrial production. The results of analysis of Pb isotopic compositions showed that in the profile, the binary mixing of two major Pb sources (parent material and vehicle exhaust), the contribution rates were 78.29% and 21.71% on average, respectively. In topsoil, at a distance of 0-7 m away from the roadside, the two sources were also parent material (75.96%) and vehicle exhaust (24.04%). At 31-300 m from the roadside, the main sources were parent material (73.85%) and coal (26.15%). The combined Pb-Sr isotope tracing pollution sources confirm the Pb isotope analysis.

1. Introduction

Roads play a major role in stimulating social and economic progress. Rapid urbanization, unregulated industrialization, and growing transport intensity have created problems of metal contamination of soils surrounding the urban roads. Many studies have been performed on metal contamination of roadside soils around the world (Kadi, 2009; Dao et al., 2010; Qian et al., 2011). Roadside soils have long been known to contain high levels of metals. Generally, the influence of traffic on soil contamination decreased with increasing soil depth and distance to the road (Werkenthin et al., 2014).

In addition, a large number of studies have been devoted to determining the sources of metals in roadside soils. The pollution sources of metals in the environment are mainly derived from anthropogenic sources. The origin of metals in the roadside soil is generally linked to traffic emission particles (originating from vehicle exhaust, tire wear, weathered street surface, and brake lining wear), industrial emission (i.e., power plants, coal combustion, metallurgical industry, auto repair shops, and chemical plants), and domestic emissions, weathering of building and pavement surfaces and atmospheric deposited particles (Oliva and Espinosa, 2007; Sindern et al., 2007; Morton-Bermea et al., 2009; Kumar et al., 2013). Multivariate statistical analysis and isotope tracing methods have been widely used to determine the sources of metal pollution in soil (Lee et al., 2006; Martinez et al., 2008; Klaminder et al., 2011; Kayhanian, 2012). As risk assessment is the essential foundation of risk management, it is important to develop a reliable approach to quantitatively assess risk to human health posed by metals. It is desperate state of the metal pollution that the government and the people are more concerned in China. Therefore, it is of great significance to carry out health risk assessment of metals in the roadside soil.

The purpose of this investigation is to determine the concentration of 26 different metals in the roadside soil (topsoil and profile soil) to assess the contamination levels of the metals. Multivariate statistical analysis and Pb-Sr isotope tracing techniques were used to study the source of metal pollution in roadside soil.

* Corresponding author at: College of Chemical Engineering, Huaqiao University, Xiamen 361021, China.
E-mail address: grhu@hqu.edu.cn (G. Hu).

http://dx.doi.org/10.1016/j.geoderma.2017.06.017
Received 28 September 2016; Received in revised form 15 June 2017; Accepted 16 June 2017
Available online 27 June 2017

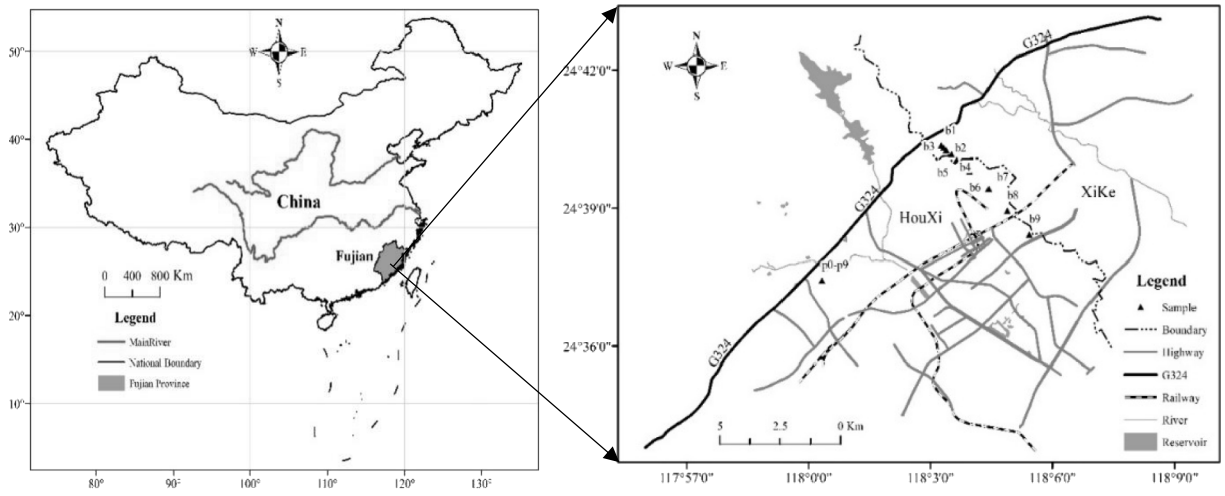

Fig. 1. Sample locations of soils along the G324 roadside.

2. Materials and methods

2.1. Study site

The territory studied in this paper is the Houxi Avenue (Xiamen, Fujian Province) of the southeast of China. The G324 is a national highway in China, the starting point is in Fuzhou in Fujian Province and the destination is Kunming in Yunnan Province, with a full length of 2712 km. The road, completed in 1936, passes through five provinces (Fujian, Guangdong, Guangxi, Guizhou and Yunnan). This road is one of the important traffic arteries in the city of Xiamen and is a transportation hub between Xiamen Island and the four districts outside of Xiamen Island.

Xiamen located at the mouth of the Jiulong River, southeast China. It has been designated a special economic development city, in part because of its key position across the Taiwan Strait from Taiwan. It has a subtropical marine climate, which is mild and rainy and there is substantial hilly land, which are mainly composed of red soil, and the plain area is mainly paddy soil (Chen et al., 2010a).

Sampling points were set in the location of the road away from the industrial area (Fig. 1). We analyzed 26 elements (Li, Be, Sc, V, Cr, Co, Ni, Cu, Zn, Ga, Rb, Sr, Y, Mo, Cd, In, Sb, Cs, Ba, Tl, Pb, Bi, Th, U, Fe and Mn) in soil samples and their distribution characteristics. Enrichment factors, potential ecological risk index and human health risk assessment were used to evaluate the metal pollution levels. Principal component analysis, hierarchical cluster analysis and the Pb-Sr isotope tracing technique were used to trace the sources of metals.

2.2. Sample collection and preparation

Topsoil (0–20 cm) was collected from the edge of roads to locations about 1, 3, 7, 15, 31, 63, 127, and 300 m from the edge of the road (0 m). Vertical profiles through the soil horizons were extracted using a cylindrical layered profile sampler, collecting 10 cm per layer thickness. All samples were carefully stored in a clean plastic vessel prior to processing and analysis, and labeled with the sampling location, date, number, and person collecting the sample. In the laboratory, soil samples were air-dried in a controlled clean environment and litter, roots, animal residues, and other debris were removed. The soil was then spread into a thin layer and repeatedly turned to accelerate drying. The samples were then ground with an agate pestle and mortar sieved with a 74 μm nylon sieve. The material under the sieve was stored in polyethylene sealed bags for future analysis, and the sieve materials were returned to the original bag.

2.3. Sample analysis

2.3.1. Total metals testing

All soil samples were analyzed using microwave digestion with HCl-HNO_3-HF (Wysocka and Vassileva, 2016). Fe, Mn were analyzed by Atomic absorption spectrometer (AAS, TAS-986, Beijing's general instrument co., LTD) and other metals were analyzed by inductively coupled plasma-mass spectrometry. The procedure applied for the preparation of the blend solutions was the following: about 0.1 g soil sample, adequate volumes of the complex digestive solutions: 4 mL of HNO_3, 0.1 mL of HCl, and 1 mL of HF were subsequently added into each Teflon vessel followed by samples digestion in the closed microwave system. The 5-steps microwave digestion program was applied: I) 5 min ramp time from 0 to 300 W and 5 min hold time; II) 2 min ramp time to 600 W and 2 min hold time; III) 2 min ramp time to 1200 W and 10 min hold time; IV) 2 min ramp time to 600 W and 15 min hold time; V) 20 min cooling time. After sample digestion Teflon vessels were placed on a ceramic heating plate and evaporated to near dryness. The final residues were dissolved in 0.14 $mol \cdot L^{-1}$ HNO_3, then quantitatively transferred to 50 mL PE bottles and finally stored at 4 °C. Rh element was used to be the internal standard. Sample solutions and reagent blanks were analyzed for metals using inductively coupled plasma-mass spectrometry (ELAN9000, Perkin-Elmer, USA) at the Chinese Academy of Sciences. Background corrections and matrix interference were monitored throughout the analyses. All experiments involving the soil samples were conducted in duplicate.

2.3.2. Measurement of Pb isotopes

Digestion of total Pb isotopic ratios: 0.1 g of soil sample was placed into the sample cup, followed by the addition of 1 mL of HNO_3 and 2 mL of HF. The cup was then sealed and placed on the heating plate for digestion at 180 °C for 4 h. The solution was removed after the sample was fully digested and the solution became clear. The cup was then unsealed and evaporated after it had cooled. 1 mL of HCl was added, and the solution was heated until it was fully evaporated. Exactly 1.5 mL of 0.5 $mol \cdot L^{-1}$ HBr was added to the sample cup, which was then sealed and heated for 1 h. After the sample was completely redissolved, the sample solution was then transferred to a 1.5 mL centrifuge tube after it had cooled, which was then centrifuged for 5 min at 10000 $r \cdot min^{-1}$.

Isolation and purification of lead isotopes: the supernatant of the centrifuged solution was transferred into a PTFE ion exchange column packed with Bio-Rad AG1-X1 anion exchange resins (200 mesh) that has been washed with 0.25 $mol \cdot L^{-1}$ HBr. Subsequently, 1.5 mL of 7.2 $mol \cdot L^{-1}$ HCl was added slowly to the filtration column in batches, and a clean PTFE cup was used to receive the filtrate. The filtrate was

then heated until only about 1 drop of solution remained in the cup. The drop was transferred to the PTFE ion exchange column and purified again, using the same procedures described above. Finally, one drop of HNO3 was added to the evaporated extract, which was then dried to convert it into a HNO3 system. This solution was then sealed to further measurement. The Pb separation and purification was conducted using the analytical procedure GB/T 17672-1999 (Determinations for isotopes of lead, strontium and neodymium in rock samples).

Digestion of acid-extractable Pb contents and isotopic ratios: 0.2 g of soil sample was placed into the sample cup, followed by the addition of 5 mL, 0.5 mol/L HNO_3, then vibrated extraction for 16–24 h, at 22 ± 5 °C, centrifuged for 10 min at 4000 r·min^{-1}. The supernatant of the centrifuged solution was transferred into a 50 mL, and centrifuged supernatant filtration, and then transferred to a 50 m L volumetric flask. Washed the residue 3 times by 3% HNO_3, centrifuged then transferred the supernatant to the volumetric flask. After diluted to 50 mL by 3% HNO_3, the acid-extractable Pb contents were determined by ICP-OES. The digestion solution was diluted to 25 ppb by 5% HNO_3, and the ratio of acid-extractable Pb isotope was determined by ICP-MS.

2.3.3. Measurement of Sr isotopes

Sample digestion: Similar to the isolation and extraction of lead isotopes, after the sample was fully digested in the sample cup, the solution was unsealed for evaporation until it had cooled. 1 mL of HCl was then added and repeated three times. After then, 1.5 mL of 0.5 mol·L^{-1} HCl was accurately pipetted into the sample cup, and the cup was then sealed and heated to allow the sample to re-dissolve. After the sample solution had cooled, it was transferred to a 1.5 mL centrifuge tube, and centrifuged for 10 min at 10000 r·min^{-1}.

Isolation and purification of strontium isotopes: After the sample was centrifuged, the supernatant was transferred into a PTFE ion exchange column (resin: Dowex 50 W). 33 mL of 2.0 mol·L^{-1} HCl was added to the ion exchange column in batches, followed by the addition of 2 mL of 3.0 mol·L^{-1} HCl. A small and clean quartz cup was used to collect the column's eluate, to which 6 mL of 3.0 mol·L^{-1} HCl was added. The quartz cup containing the eluate was heated at 150 °C and then 1 mL of double-distilled water was added before it was transferred to the ion exchange column again. The sample-containing quartz cup was then dried on the heating plate, and sealed to further measurement.

2.3.4. Experimental quality control

Preparation of Pb and Sr isotope ratio samples was conducted in a clean laboratory in the Analytical Laboratory Beijing Research Institute of Uranium Geology, and determined using VG354 thermal ionization mass spectrometry, solutions of reference materials (NBS981 for Pb isotope and NBS987 for Sr isotope, National Bureau of Standards, USA) were determined before every five samples as standards for calibration and quality control. The acids used for digestion were all metal-oxide-semiconductor (MOS).

3. Results and discussion

3.1. Total metal level

Metal concentrations in the topsoils and profile soil were showed in Table 1. In vertical profiles, Cu, Zn, Rb, Sr, Cd, In, Ba, and Pb showed accumulation in topsoil, the other metals were irregular. In topsoils, the maximum values of Be, Ga, Rb, Y, Tl, Th, and U were at 3 m, excluding the Ba observed at 15 m, all other metals appeared within 3 m from the road, which suggests that these metals were sourced from road traffic. This was consistent with the results of Chen et al. (2010b) and Azeez et al. (2014).

3.2. Pollution assessment of metals.

3.2.1. Enrichment factors (EFs)

The EFs were calculated to determine the anthropogenic input of metals in soils following Dantu (2009). The EFs can be used to evaluate the degree of anthropogenic influence on soil contamination by metals, and to differentiate the metals originating mainly from human activities from those of natural sources (Ye et al., 2011). The value of *EFs* can be calculated using the Eq. (1):

$$\mathrm{EF} = \frac{(\mathrm{C_i}/C_{Fe})_s}{(\mathrm{C_i}/C_{Fe})_r} \quad (1)$$

where EF is the enrichment factor of an element, $(C_i/C_{Fe})_s$ is the ratio of the concentration of an element with that of Fe at each sampling point, and $(C_i/C_{Fe})_r$ is same ratio of the background content in soils. In this case, the element concentrations in the depth profile of 100 cm (p9) were consistent with those in a plateau, which can be extrapolated as background values in our study (Carrero et al., 2013). Soils were categorized into seven classes based on the value of *EF* as follows: $EF < 1$ indicates no enrichment, $EF < 3$ indicates minor enrichment, *EF* of 3–5 indicates moderate enrichment, *EF* of 5–10 indicates moderate-to-severe enrichment, *EF* of 10–25 indicates severe enrichment, *EF* of 26–50 indicates very severe enrichment, and $EF > 50$ indicates extremely severe enrichment (Ali et al., 2015). Iron (Fe) was used for geochemical normalization and shale reference values were taken after Turekian and Wedepohl (1961).

The EF values in the profile and topsoil are depicted in Fig. 2A and Fig. 2B. Except for Cu (0-10 cm), which was severe enrichment, all the other metals showed minor enrichment and moderate enrichment in the profile soil. Obviously, the EFs of topsoil were greater than the value of profile soil. In topsoils, the average EF of Cd, which was the largest, reached the degree of severe. This may be attributed to the traffic factors. Therefore, surface soils were mainly influenced by the traffic factors; however, this effect weakens with the increase of soil depth.

3.2.2. Potential ecological risk index

The potential ecological risk index (*RI*) was introduced by Hakanson (1980) to assess the degree of ecological risk of metals in soil or sediments and has been widely used (Yang et al., 2009). The value of *RI* can be calculated by Eqs. (2)–(4) (Hakanson, 1980):

$$C_f^i = \frac{C_D^i}{C_n^i} \quad (2)$$

$$E_r^i = T_r^i C_f^i \quad (3)$$

$$RI = \sum_{i=1}^{n} E_r^i \quad (4)$$

where $E_r{}^i$ is the potential risk of individual metal; $T_r{}^i$ is the toxic-response factor for a given metal, the toxic-response factor for Mn and Zn was 1, V and Cr was 2, whereas Cu, Pb, Ni and Co was 5, and Cd was 30 (Hakanson, 1980); $C_f{}^i$ is the contamination coefficient; $C_D{}^i$ is the present concentration of metals; $C_n{}^i$ is the background content of metal in soils. Hakanson (1980) defined five categories of $E_r{}^i$, and four categories of *RI*, as follows: $E_r{}^i < 40$ or $RI < 150$ indicates low risk, $E_r{}^i$ of 40–80 or *RI* of 150–300 indicates moderate risk, $E_r{}^i$ of 80–160 or *RI* of 300–600 indicates considerable risk, $E_r{}^i$ of 160–320 indicates considerable risk, $E_r{}^i \geq 320$ or $RI \geq 600$ indicates very high risk (Wu et al., 2010). The ecological risk assessment results of toxic metals in soils of roadside are shown in Fig. 2C and Fig. 2D. We found that the $E_r{}^i$ of metals were ranked in the order of Cd > Cu > Ni > Pb > Co > Cr > V > Mn > Zn and Cd > Cu > Pb > Co > Ni > Mn > Zn > Cr > V in the profile soil and topsoil, respectively. This indicates that the *RI* assessment results were mainly associated with the content of Cd in soil. This is probably because the $T_r{}^i$ value for Cd is substantially higher than

Table 1
Metal concentrations in the topsoils and profile soil (mg·kg^{-1})[a].

	Depth (cm)	Li	Be	Sc	V	Cr	Co	Ni	Cu	Zn	Ga	Rb	Sr	Y	Cd	Mo	Fe	Mn	In	Sb	Cs	Ba	Tl	Pb	Bi	Th	U
p0	0–10	14.00	1.010	8.390	52.50	26.40	3.000	17.20	157.0	163.0	16.00	74.30	41.40	21.80	0.144	2.930	20,179	768.0	0.157	0.728	3.810	320.0	0.543	53.40	0.998	31.70	6.730
p1	10–20	16.10	1.610	9.330	56.40	27.00	3.680	16.40	12.20	60.30	18.60	62.40	26.50	23.00	0.059	2.550	19,130	777.5	0.121	0.634	4.830	196.0	0.603	44.20	1.020	35.70	7.640
p2	20–30	18.80	1.210	10.10	71.30	33.50	4.090	19.50	10.50	66.80	22.50	61.70	23.20	22.20	0.081	2.800	28,540	557.3	0.118	0.678	5.880	170.0	0.692	38.40	1.130	35.30	7.620
p3	30–40	21.70	1.320	10.80	69.40	33.30	4.870	18.20	10.70	64.20	25.00	60.00	23.20	16.90	0.043	2.340	22,172	508.5	0.113	0.581	6.380	155.0	0.638	40.40	1.140	30.10	7.020
p4	40–50	20.80	1.290	11.10	78.00	35.70	4.980	19.40	10.70	63.40	25.70	63.70	24.80	19.80	0.059	3.130	25,126	473.3	0.114	0.712	6.760	156.0	0.747	43.00	1.210	31.50	7.410
p5	50–60	21.50	1.320	6.530	81.60	37.40	5.080	22.20	13.50	71.10	25.20	64.50	24.10	16.30	0.045	2.990	27,151	424.3	0.122	0.724	6.800	152.0	0.738	45.30	1.200	27.90	6.720
p6	60–70	19.50	1.340	6.650	58.50	35.00	4.790	19.70	11.70	70.50	25.70	61.10	21.80	17.00	0.064	0.257	24,752	357.0	0.094	0.036	6.490	138.0	0.695	44.10	1.210	27.30	6.730
p7	70–80	23.10	1.370	11.90	88.50	39.30	5.970	21.20	12.40	67.00	28.60	69.30	24.50	22.00	0.056	3.540	28,990	352.0	0.130	0.835	7.550	158.0	0.799	45.00	1.290	32.30	7.470
p8	80–90	20.60	1.450	11.20	92.10	36.70	4.830	19.40	11.80	70.20	28.50	68.50	22.40	17.50	0.076	3.260	34,918	321.5	0.125	0.760	7.120	144.0	0.779	45.20	1.340	26.20	7.340
p9	90–100	19.30	1.560	9.880	73.40	33.30	4.450	18.60	13.10	85.10	28.30	63.80	21.20	18.80	0.036	0.957	32,894	283.8	0.112	0.498	6.420	139.0	0.700	42.90	1.170	30.90	7.130
Minimum		14.00	1.010	6.530	52.50	26.40	3.000	16.40	10.50	60.30	16.00	60.00	21.20	16.30	0.036	0.257	19,130	283.8	0.094	0.036	3.810	138.0	0.543	38.40	0.998	26.20	6.720
Maximum		23.10	1.610	11.90	92.10	39.30	5.970	22.20	157.0	163.0	28.60	74.30	41.40	23.00	0.144	3.540	34,918	777.5	0.157	0.835	7.550	320.0	0.799	53.40	1.340	35.70	7.640
Mean		19.54	1.348	9.588	72.17	33.76	4.574	19.18	26.36	78.16	24.41	64.93	25.31	19.53	0.066	2.475	26,385	482.3	0.121	0.619	6.204	172.8	0.693	44.19	1.171	30.89	7.181
CV%		13.97	12.68	19.52	18.59	12.42	17.99	8.966	174.2	39.09	17.37	6.857	23.16	13.10	46.30	42.59	19.59	36.34	13.33	36.46	17.98	31.49	11.50	8.884	9.092	10.24	5.111
	Distance(m)	Li	Be	Sc	V	Cr	Co	Ni	Cu	Zn	Ga	Rb	Sr	Y	Cd	Mo	Fe	Mn	In	Sb	Cs	Ba	Tl	Pb	Bi	Th	U
b1	0	11.00	2.400	7.110	49.50	54.00	6.580	14.10	46.70	269.0	14.30	127.0	190.0	29.80	0.689	3.510	24,485	754.5	0.122	1.320	3.400	558.0	0.634	76.40	0.894	37.00	6.700
b2	1	12.00	3.310	6.270	42.40	40.40	7.670	13.20	72.50	290.0	17.60	162.0	183.0	30.60	0.468	6.310	22,986	737.0	0.103	0.802	3.020	560.0	0.784	73.80	0.925	52.60	11.20
b3	3	9.060	3.580	6.400	31.10	23.00	5.460	8.130	26.90	191.0	17.30	176.0	135.0	29.70	0.434	2.420	13,470	604.5	0.128	0.668	2.300	544.0	0.781	56.70	1.200	48.10	14.70
b4	7	7.400	3.340	6.900	29.40	19.10	4.250	7.600	16.20	90.90	18.80	193.0	114.0	31.50	0.324	6.020	13,264	550.8	0.090	0.398	2.300	519.0	0.820	41.10	0.650	50.70	11.40
b5	15	6.900	2.120	6.640	28.40	15.00	3.550	5.840	10.30	44.60	20.90	263.0	70.10	37.80	0.101	1.910	8485.0	388.3	0.098	0.262	2.770	655.0	1.190	41.20	0.527	35.80	11.00
b6	31	8.010	3.480	9.410	28.10	11.80	3.040	5.010	6.850	44.70	23.90	268.0	69.00	38.10	0.163	3.190	4845.0	367.0	0.086	0.223	3.060	531.0	1.310	39.90	0.538	69.40	15.00
b7	63	6.920	2.160	8.000	28.00	13.50	2.650	4.730	8.070	42.90	17.60	215.0	74.50	21.00	0.179	2.040	5544.0	472.8	0.081	0.375	2.940	577.0	1.070	36.90	0.753	31.40	8.750
b8	127	5.360	1.480	5.760	26.00	18.10	2.390	5.170	13.10	50.10	15.30	220.0	68.60	21.70	0.187	1.280	8012.0	439.3	0.087	0.308	2.600	541.0	1.020	40.50	0.615	36.40	8.910
b9	300	6.900	1.780	8.860	35.40	14.50	5.160	9.620	24.80	86.40	18.20	171.0	52.60	25.20	0.315	1.960	15,773	532.8	0.070	0.490	2.950	463.0	0.989	42.90	0.885	32.80	7.230
Minimum		5.360	1.480	5.760	26.00	11.80	2.390	4.730	6.850	42.90	14.30	127.0	52.60	21.00	0.101	1.280	4845.0	367.0	0.070	0.223	2.300	463.0	0.634	36.90	0.527	31.40	6.700
Maximum		12.00	3.580	9.410	49.50	54.00	7.670	14.10	72.50	290.0	23.90	268.0	190.0	38.10	0.689	6.310	24,485	754.5	0.128	1.320	3.400	655.0	1.310	76.40	1.200	69.40	15.00
Mean		8.172	2.628	7.261	33.14	23.27	4.528	8.156	25.05	123.3	18.21	199.4	106.3	29.49	0.318	3.182	12,985	538.5	0.096	0.538	2.816	549.8	0.955	49.93	0.776	43.80	10.54
CV%		26.23	30.59	17.03	23.90	61.81	40.35	43.16	86.81	81.21	15.69	23.42	49.09	20.76	59.00	57.26	54.93	25.99	19.71	64.83	12.91	9.303	22.83	30.69	28.40	28.41	28.09

[a] The RSD of all metals was < 6%.

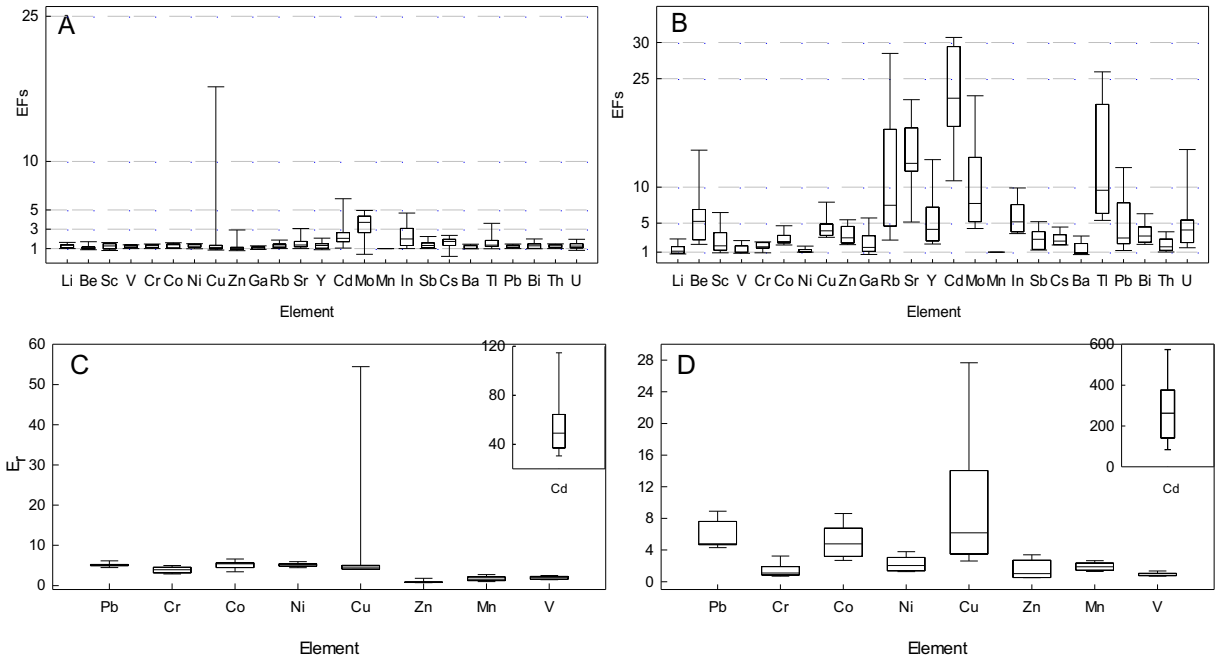

Fig. 2. Pollution assessment of metals at the roadside. A) enrichment factors in profile soil; B) enrichment factors in topsoil; C) box-and-whisker plots of the potential ecological risk index in profile soil; D) box-and-whisker plots of the potential ecological risk index in topsoil.

that of other elements (Hakanson, 1980). The very high risk to environments posed by Cd should give rise to widespread concerns. In addition, in the surface soil at the roadside, a great contribution of *RI* was attributed to Pb, Ni and Cu, which may also be affected by the traffic pollution sources, with a moderate ecological risk.

3.2.3. Human health risk assessment

Human health risk assessment of metals in soils is related to hazard discrimination, exposure evaluation, and risk characterization (Meza-Montenegro et al., 2012; Wu et al., 2015). In consideration of potential toxicity and carcinogenicity of most elements, carcinogenic and non-carcinogenic effects of metals were both studied. In this study, three exposure ways of metals to human body were considered: (a) direct oral ingestion of soil particles (ADD_{ing}); (b) dermal absorption of elements in soils adhered to exposed skin (ADD_{dermal}); and (c) inhalation of resuspended soil particulates by nose or mouth (ADD_{inh}). The methodology used in this study to calculate the exposure risks of soil metals posed to the public is based on those developed by the United States Environmental Protection Agency for health risk assessment (USEPA, 1989, 2001). The dose received through ingestion, dermal and inhalation absorption can be respectively estimated by (USEPA, 1989).

Cu, Zn, Pb, Ni, Cr, Cd were chosen for the health risk assessment. Cr and Cd have carcinogenic risk (Fang et al., 2015), and others are non-carcinogenic risks. The population were divided into two parts, adults and children, in this paper. One population group that could potentially be more highly exposed to inhalation exposures at a site is children. As discussed by EPA (2009), exposure parameters related to activity patterns (e.g., exposure time, frequency, and duration) and MEs, may vary across age groups. For example, due to outdoor play patterns, children may spend more time near the source of contamination than adults, and thus would have higher exposure time and/or exposure frequency values than adults living in the same location. Therefore, it is important to carefully describe site-specific exposures to children, and assumptions made in risk calculations. The definition and reference values for all parameters are listed in Table 2.

Exposure dose was calculated using Eqs. (5)–(7). The results were shown in Table 3.

Direct oral ingestion of soil particles (ADD_{ing}):

$$ADD_{ing}\,(mg{\cdot}kg^{-1}{\cdot}d^{-1}) = C\,(mg{\cdot}kg^{-1}) \times \frac{IngR \times EF \times ED}{BW \times AT} \times 10^{-6} \quad (5)$$

Dermal absorption of elements in soils adhered to exposed skin (ADD_{dermal}):

$$ADD_{inh}\,(mg{\cdot}kg^{-1}{\cdot}d^{-1}) = C\,(mg{\cdot}kg^{-1}) \times \frac{IngR \times EF \times ED}{PEF \times AT \times BW} \quad (6)$$

Inhalation of resuspended soil particulates by nose or mouth (ADD_{inh}):

$$ADD_{dermal}\,(mg{\cdot}kg^{-1}{\cdot}d^{-1}) = C\,(mg{\cdot}kg^{-1}) \times \frac{SA \times SL \times ABS \times EF \times ED}{BW \times AT} \times 10^{-6} \quad (7)$$

where ADD_{ing}, ADD_{dermal} and ADD_{inh} are the average daily intake from soil ingestion, dermal and inhalation absorption, respectively ($mg{\cdot}kg^{-1}{\cdot}d^{-1}$), C is the concentration of metal in soil ($mg{\cdot}kg^{-1}$).

The doses calculated for each element and exposure pathway are subsequently divided by the toxicity threshold value which is referred to as the reference dose (RfD, $mg{\cdot}kg^{-1}{\cdot}d^{-1}$) (Table 3) of a specific chemical to yield a non-carcinogenic hazard quotient (HQ), whereas for carcinogens the dose is multiplied by the corresponding slope factor (SF) to produce a level of cancer risk (Ferreira-Baptista and De Miguelb, 2005). To assess the overall potential for non-carcinogenic effects posed by all exposure pathways, a Hazard Index (HI) which is the total non-carcinogenic risk of exposure to a variety of pollutants has been employed as described by Eq. (8) (USEPA, 1989; Li et al., 2014). If $HQ < 1$ or $HI < 1$, the exposed individual is unlikely to experience obvious adverse health effect. On the contrary, if $HQ > 1$ or $HI > 1$, there is a chance that non-carcinogenic effect may occur with a probability which tends to increase as HI increases (Man et al., 2010).

$$HI = \sum HQ_i = \sum \frac{ADD_i}{RfD_i} \quad (8)$$

Generally, carcinogenic risk is regarded as the probability of an individual developing any type of cancer in the whole life time due to exposure to carcinogenic hazards (Li et al., 2014). Similarly, the aggregate carcinogenic risk (Risk) is calculated by summing the individual cancer risk across all exposure pathways using Eq. (9).

Table 2
Definition and reference value of some parameters for health risk assessment of metals in soils.

Symbol (units)	Parameter	Value	References
IngR ($mg{\cdot}day^{-1}$)	Soil ingestion rate	200 (children);100 (adult)	US EPA, 2001
InhR ($mg{\cdot}day^{-1}$)	Soil inhalation rate	7.6 (children);20 (adult)	Ferreira-Baptista and De Miguelb, 2005
EF ($d{\cdot}a^{-1}$)	Exposure frequency	180	Ferreira-Baptista and De Miguelb, 2005
ED (a)	Exposure duration	6 year(children);24 year(adult)	US EPA, 1996, 2001
BW (kg)	Body weight	15 (children);70 (adult)	US EPA, 1996, 2001
SA (cm^2)	Exposed skin surface area	1150 (children);2145 (adult)	Wang et al., 2008
SL ($mg{\cdot}cm^{-2}{\cdot}day^{-1}$)	Adherence factor AF	0.2 (children);0.07(adult)	US EPA, 1996, 2001
ABS (unitless)	Dermal absorption factor	0.001	US DOE, 2004
AT (day)	Average time	ED × 365(non-carcinogenic); 70 × 365(carcinogenic)	US EPA, 1989
PEF ($m^3{\cdot}kg^{-1}$)	emission factor	1.36×10^9	US EPA, 2001

$$Risk = ADD \times SF \quad (9)$$

As shown in Table 3, the results of 6 kinds of metals in three exposure ways, both children and adults are as follows: direct oral ingestion of soil particles is the highest, followed by dermal absorption of elements in soils adhered to exposed skin and inhalation of resuspended soil particulates by nose or mouth minimization. The results are consistent with Chang et al. (2009) and Ferreira-Baptista and De Miguelb (2005). Children's exposure risk to Pb is the highest, HQ reached 0.0831, by direct oral ingestion of soil particles. Compared profile with surface soil, exposure risk of Pb, Cd, Zn in surface soil is greater than that in the profile soil, Ni, Cr, Cu are on the contrary. The results of the HI values of the 6 kinds of metals were Pb > Cr > Ni > Cu > Zn > Cd, both for children and adults. The HQ and HI were higher in children than in adults, showed that the non-carcinogenic risk of children was higher than that of adults. But whether children or adults, HQ and HI of all kinds of metals in different exposure ways were < 1, which indicate the risk is small or negligible, could not cause obvious health hazards on the surrounding population. But need to be vigilant against Pb in surface soil direct oral ingestion of soil particles on children's noncarcinogenic risk. Cd and Cr on children's cancer risk was slightly higher than that of adults, but their risk values are in acceptable carcinogenic risk value range (10^{-7}–10^{-4}), indicating that the Cd and Cr in the roadsides soil has not been on urban residents caused by carcinogenic risk.

3.3. Source analysis of metal elements by multivariate statistical analysis

3.3.1. Principal component analysis (PCA)

Principal component analysis (PCA) technique was applied to infer the hypothetical source of heavy metals(natural or anthropogenic). PCA was performed by varimax rotation. Varimax rotation was employed because orthogonal rotation minimizes the number of variables with a high loading on each component and therefore facilitates the interpretation of PCA results. This technique clusters variables into groups such that variables belonging to one group are highly correlated with one another. The values of principal components (PCs) can be calculated based on the contents of metals in soils and the contamination levels of metals in soil can be assessed by weight sum of different principal component values. The PCA results of heavy metal contents calculated by SPSS 19.0 were shown in Fig. 3A and Fig. 3B.

Three PCs led to a reduction of the initial dimensions of the dataset to three components, which explained 86.00% and 83.73% of the data variation in the profile and the topsoil, respectively. Therefore, these three factors played a significant role in explaining metal contamination in the study area.

For profile soils (Fig. 3A), the first principal component (PC1) spanning the greatest amount of variance (40.84%), included Ba, In, Sr, Cu, Cd, Zn, Pb and Rb, suggesting that these elements share the same origin. Pb, Cu, Cd, Zn were generally associated with traffic activities (Gunawardena et al., 2014 and 2015). The Pb had a positive loading, which indicates that it was influenced by traffic activities, though leaded fuel had been phased out in Xiamen over a decade ago. Therefore, the positive loading was primarily attributed to the re-suspension of Pb from past emissions from fuel combustion deposited in soil and its disturbance by traffic activities. We suggest that Zn and Cd originates from automobile tire wear and lubricating oil burning (Sawyer et al., 2000). Additionally, guardrails on the highway have also been considered as an important source of Zn in topsoils (Carrero et al., 2012). The degradation of the brake lining not only causes pollution of Cd and Pb, but also Cu (Harrison et al., 2003). Barium is used as filler in the form $BaSO_4$ to reduce manufacturing costs and to improve manufacturability of the brake lining (Thorpe and Harrison, 2008). In several works brake wear was identified as the major source of high Barium concentration values in atmospheric particulate and road dust samples. Sr and Ba are widely used in alloy (Zhang et al., 2015). In this work, we therefore suggest as the representative pollutant source of PC1 the “traffic”. The second principal component (PC2) accounted for 29.46% of the variance and had high loadings for Fe, Ni, Bi, V, Li, Cr, Ga, Co, Cs, and Tl. Ni and V, in association, are usually recognized as a marker of fuel oil combustion and petrochemical plants emission (Hedberg et al., 2005; Jang et al., 2007; Querol et al., 2007; Mazzei et al., 2008; Rajsi et al., 2008). The main source of Cs was the pharmaceutical and electronics industries (Dong and Xiao, 2005), Ni and Cr mainly come from the electronic screen manufacturing, alloy production, metal smelting industries. The main types of industry in the study area are TV manufacturers and metal processing enterprises (Sun et al., 2016). In this paper, we suggest as the representative pollutant source of PC2 the “industry”. The third principal component (PC3) represented 15.70% of variance and high positive loadings of basic cations such Mn, Y, Th, U, Sc, Be, Sb, and Mo. We attribute PC3 to natural sources and suggest that these metals originated from parent rocks.

For topsoil (Fig. 3B), PC1 represented the greatest amount of variance (57.97%) and included Ni, Fe, V, Co, Cu, Cd, Sb, Mn, Zn, Pb, Sr, Cr, Li, In, and Bi, indicated that these elements shared the same origin. The ratio of average content to the background of Cd (8.83), which is the highest in all metals, indicated the most serious pollution. Pb, Cd, Cu, Zn, Ba are the characteristic elements of traffic pollution, according to the previous discussion. On the one hand, Fe and Mn are common in the natural environment (rocks and soils) and can originate from erosion processes. On the other hand, the literature data indicates a possible anthropogenic source of both metals (Adamo et al., 2011). High content of Fe and Mn is usually found in the tire linings and in the dust originated from brakes and engines. Moreover, Fe oxides are used as the abrasion agents in brake linings (Wawer et al., 2015). However there is no sufficient evidence to show that the rest of the elements relate to traffic pollution, further research is required. The PC2 accounted for 16.86% of the variance and had high loadings for Be, Th, U, Y, Mo shared the same origin. Th, Y, U existed in granite (Nardi et al., 2013), indicated the dominance of lithogenic elements. Molybdenum trioxide is an inorganic filler that prevents thermal fade and cracking of friction lining under high temperature conditions (Chan and Stachowiak, 2004), but it is also used as an additive to impart special qualities to the

Table 3
Non-carcinogenic and carcinogenic risks for two populations due to environmental exposure to soil metal.

Non-carcinogenic risks

Populations	Met-als	ADD_{ing}		ADD_{inh}		ADD_{dermal}		RfD_{ing}*	RfD_{inh}*
		Profile	topsoils	Profile	topsoils	Profile	topsoils	($mg{\cdot}kg^{-1}{\cdot}d^{-1}$)	
Children	Cr	2.22×10^{-4}	1.53×10^{-4}	6.20×10^{-9}	4.27×10^{-9}	2.55×10^{-7}	1.76×10^{-7}	5.00×10^{-3}	2.86×10^{-5}
	Ni	1.26×10^{-4}	5.36×10^{-5}	3.52×10^{-9}	1.50×10^{-9}	1.45×10^{-7}	6.17×10^{-8}	2.00×10^{-2}	2.06×10^{-2}
	Cd	4.36×10^{-7}	2.09×10^{-6}	1.22×10^{-11}	5.84×10^{-11}	5.01×10^{-10}	2.40×10^{-9}	1.00×10^{-3}	1.00×10^{-3}
	Zn	5.14×10^{-4}	8.11×10^{-4}	1.44×10^{-8}	2.26×10^{-8}	5.91×10^{-7}	9.32×10^{-7}	3.00×10^{-1}	3.00×10^{-1}
	Cu	1.73×10^{-4}	1.65×10^{-4}	4.84×10^{-9}	4.60×10^{-9}	1.99×10^{-7}	1.89×10^{-7}	3.70×10^{-2}	4.02×10^{-2}
	Pb	2.91×10^{-4}	3.28×10^{-4}	8.12×10^{-9}	9.17×10^{-9}	3.34×10^{-7}	3.77×10^{-7}	3.50×10^{-3}	3.52×10^{-3}
Adult	Cr	2.38×10^{-5}	1.64×10^{-5}	2.38×10^{-8}	1.64×10^{-8}	3.57×10^{-8}	2.46×10^{-8}	5.00×10^{-3}	2.86×10^{-5}
	Ni	1.35×10^{-5}	5.75×10^{-6}	1.35×10^{-8}	5.75×10^{-9}	2.03×10^{-8}	8.63×10^{-9}	2.00×10^{-2}	2.06×10^{-2}
	Cd	4.67×10^{-8}	2.24×10^{-7}	4.68×10^{-11}	2.24×10^{-10}	7.01×10^{-11}	3.36×10^{-10}	1.00×10^{-3}	1.00×10^{-3}
	Zn	5.51×10^{-5}	8.69×10^{-5}	5.51×10^{-8}	8.70×10^{-8}	8.27×10^{-8}	1.30×10^{-7}	3.00×10^{-1}	3.00×10^{-1}
	Cu	1.86×10^{-5}	1.76×10^{-5}	1.86×10^{-8}	1.77×10^{-8}	2.79×10^{-8}	2.65×10^{-8}	3.70×10^{-2}	4.02×10^{-2}
	Pb	3.11×10^{-5}	3.52×10^{-5}	3.12×10^{-8}	3.52×10^{-8}	4.68×10^{-8}	5.28×10^{-8}	3.50×10^{-3}	3.52×10^{-3}

Non-carcinogenic risks

Populations	RfD_{derm}*	HQ_{ing}		HQ_{inh}		HQ_{dderm}		HI	
	($mg{\cdot}kg^{-1}{\cdot}d^{-1}$)	Profile	topsoils	Profile	topsoils	Profile	topsoils	Profile	topsoils
Children	2.50×10^{-4}	4.44×10^{-2}	3.06×10^{-2}	2.17×10^{-4}	1.49×10^{-4}	1.02×10^{-3}	7.04×10^{-4}	4.56×10^{-2}	3.15×10^{-2}
	1.00×10^{-3}	6.30×10^{-3}	2.68×10^{-3}	1.71×10^{-7}	7.28×10^{-8}	1.45×10^{-4}	6.17×10^{-5}	6.45×10^{-3}	2.74×10^{-3}
	5.00×10^{-5}	4.36×10^{-4}	2.09×10^{-3}	1.22×10^{-8}	5.84×10^{-8}	1.00×10^{-5}	4.80×10^{-5}	4.46×10^{-4}	2.14×10^{-3}
	6.00×10^{-2}	1.71×10^{-3}	2.70×10^{-3}	4.80×10^{-8}	7.53×10^{-8}	9.85×10^{-6}	1.55×10^{-5}	1.72×10^{-3}	2.72×10^{-3}
	1.90×10^{-3}	4.68×10^{-3}	4.46×10^{-3}	1.20×10^{-7}	1.14×10^{-7}	1.05×10^{-4}	9.95×10^{-5}	4.78×10^{-3}	4.56×10^{-3}
	5.25×10^{-4}	8.31×10^{-2}	9.37×10^{-2}	2.31×10^{-6}	2.61×10^{-6}	6.36×10^{-4}	7.18×10^{-4}	8.38×10^{-2}	9.44×10^{-2}
Adult	2.50×10^{-4}	4.76×10^{-3}	3.28×10^{-3}	8.32 × 10–4	5.73×10^{-4}	1.43×10^{-4}	9.84×10^{-5}	5.73×10^{-3}	3.95×10^{-3}
	1.00×10^{-3}	6.75×10^{-4}	2.88×10^{-4}	6.55×10^{-7}	2.79×10^{-7}	2.03×10^{-5}	8.63×10^{-6}	6.96×10^{-4}	2.96×10^{-4}
	5.00×10^{-5}	4.67×10^{-5}	2.24×10^{-4}	4.68×10^{-8}	2.24×10^{-7}	1.40×10^{-6}	6.72×10^{-6}	4.81×10^{-5}	2.31×10^{-4}
	6.00×10^{-2}	1.84×10^{-4}	2.90×10^{-4}	1.84×10^{-7}	2.90×10^{-7}	1.38×10^{-6}	2.17×10^{-6}	1.85×10^{-4}	2.92×10^{-4}
	1.90×10^{-3}	5.03×10^{-4}	4.76×10^{-4}	4.63×10^{-7}	4.40×10^{-7}	1.47×10^{-5}	1.39×10^{-5}	5.18×10^{-4}	4.90×10^{-4}
	5.25×10^{-4}	8.89×10^{-3}	1.01×10^{-2}	8.86×10^{-6}	1.00×10^{-5}	8.91×10^{-5}	1.01×10^{-4}	8.98×10^{-3}	1.02×10^{-2}

Carcinogenic risks

Populations	Metals	ADDing		ADDinh		ADDdermal		Risk	
		Profile	topsoils	Profile	topsoils	Profile	topsoils	Profile	topsoils
Children	Cr	1.90×10^{-5}	5.30×10^{-10}	2.19×10^{-8}	1.31×10^{-5}	3.65×10^{-10}	1.51×10^{-8}	1.11×10^{-4}	9.50×10^{-6}
	Cd	3.74×10^{-8}	1.04×10^{-12}	4.30×10^{-11}	1.79×10^{-7}	4.99×10^{-12}	2.06×10^{-10}	2.75×10^{-6}	2.36×10^{-7}
Adult	Cr	8.15×10^{-6}	1.20×10^{-9}	3.06×10^{-9}	5.62×10^{-6}	8.26×10^{-10}	2.11×10^{-9}	1.19×10^{-5}	4.08×10^{-6}
	Cd	1.60×10^{-8}	2.35×10^{-12}	6.01×10^{-12}	7.67×10^{-8}	1.13×10^{-11}	2.88×10^{-11}	2.94×10^{-7}	1.01×10^{-7}

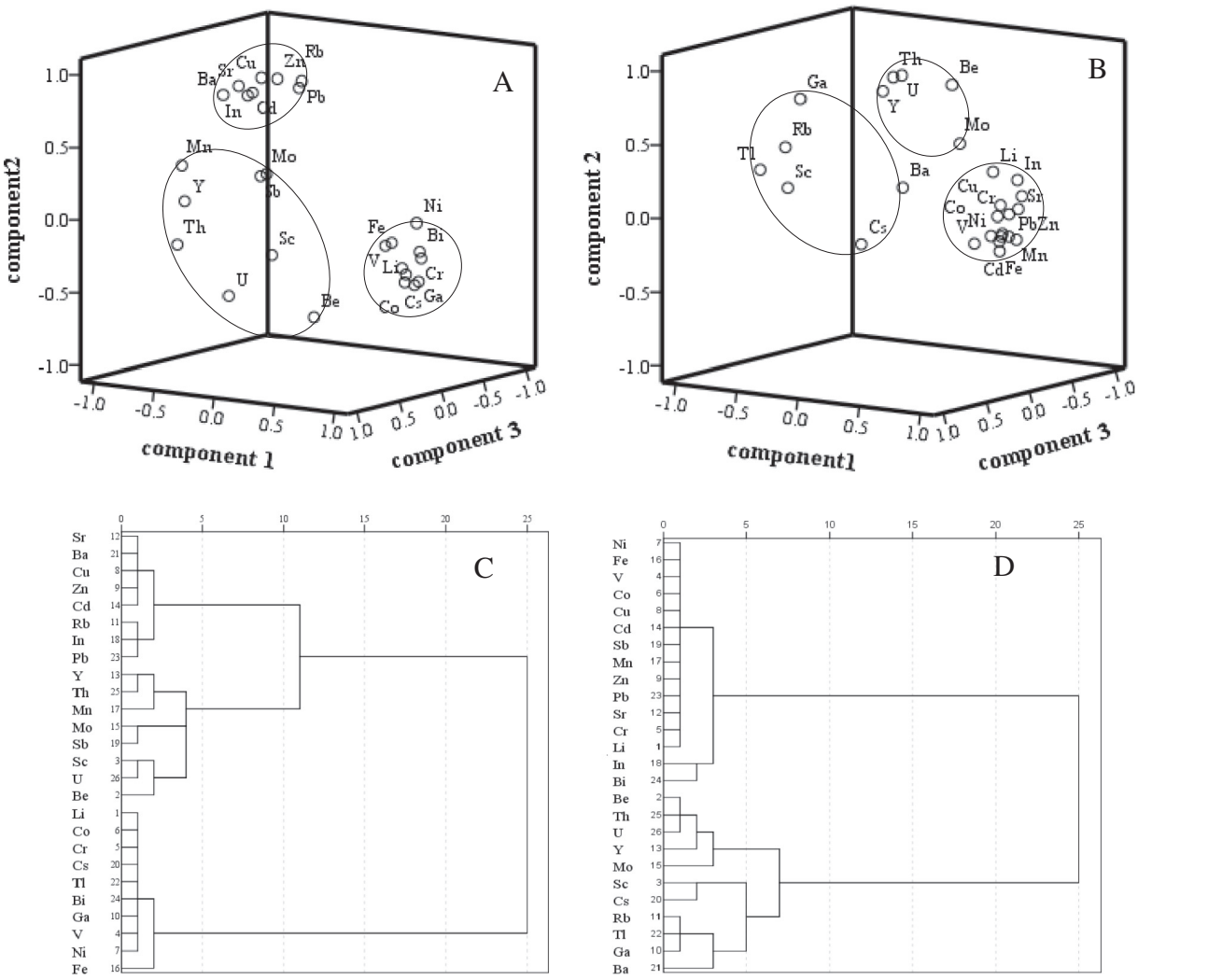

Fig. 3. Multivariate statistical analysis results of metals in the soil.
A: Loading plots of the metals contents in the space of profile soil; B: Loading plots of the metals contents in the space of topsoil; C: Hierarchical cluster analysis results of profile soil; D: Hierarchical cluster analysis results of topsoil.

oil used as lubricant and to prevent oxidation and corrosion (Fujiwara et al., 2011). Therefore, PC2 may also be affected by traffic. The PC3 represented 8.896% of the variance and high positive loadings of basic cations such Sc, Cs, Rb, Tl, Ga, Ba. The content of Rb,Tl, Ba was higher than the background value and Rb, Tl had large EFs. Usually, Rb is derived from rock weathering (Zhao et al., 2017), Tl are usually recognized as a marker of fuel oil combustion and petrochemical plants emission(as profile), Ba is related to brake wear. Therefore, PC3 may be considered as factors of natural sources and affected by anthropogenic sources in the meantime. In totally, the sources of topsoil pollution are more complex, and are basically affected by anthropogenic sources.

3.3.2. Hierarchical cluster analysis (HCA)

Cluster analysis was used to classify metals and help to identify their anthropogenic or natural sources (Li and Feng, 2012; Šajn and Gosar, 2014). In the present study, HCA was used to check results of PCA for the topsoil and the profile soils. Fig. 3C and Fig. 3D shows the results of HCA using Ward's method and Euclidean distances, the soil dataset (variables) was standardized by means of z-scores before HCA (Li et al., 2012), by SPSS 19.0. In the case of profile soil (Fig. 3C), Cluster I contained Li-Co-Cr-Cs-Tl-Bi-Ga-V-Ni-Fe (with two sub-clusters: Li-Co-Cr-Cs-Tl-Bi-Ga-V-Ni and Fe). Cluster II consisted of Sr-Ba-Cu-Zn-Cd-Rb-In-Pb-Y-Th-Mn-Mo-Sb-Sc-U- Be (with two sub-clusters: Sr-Ba-Cu-Zn-Cd-Rb-In-Pb and Y-Th-Mn-Mo-Sb-Sc-U-Be). In the case of the topsoil (Fig. 3D), Cluster I contained Ni-Fe-V-Co-Cu-Cd-Sb-Mn-Zn-Pb-Sr-Cr-Li-In-Bi (with two sub-clusters: Ni-Fe-V-Co-Cu-Cd-Sb-Mn-Zn-Pb-Sr-Cr-Li and In—Bi). Cluster II consisted of Be-Th-U-Y-Mo-Sc-Cs-Rb-Tl-Ga-Ba (with two sub-clusters: Be-Th-U-Y-Mo and Sc-Cs-Rb-Tl-Ga-Ba). Fig. 3C and Fig. 3D shows distinct clusters that were clearly separated from each other in terms of squared Euclidean distances; the long distance between them suggests that they originate from different sources. Thus, the results of HCA agreed very well with those of PCA.

3.4. Isotope tracing pollution sources

3.4.1. Lead isotope tracing pollution sources

The Pb-isotope ratio variations generally reflect a mix of several Pb sources with different isotopic signatures (Sun et al., 2011). Many studies (Cheng and Hu, 2010; Negrel and Petelet-Giraud, 2012; Townsend and Seen, 2012) have used the Pb isotope ratio characteristics to analyze pollution sources. Acid-extractable Pb isotopic signature was more sensitive than total Pb isotopic signature in identifying anthropogenic Pb sources due to the substantial variability of acid-extractable Pb isotopic ratios. In the current research, we measured the total and acid-extractable Pb isotopic compositions of the roadside soils (Table 4), and the four possible end-members (vehicle exhaust, coal, sludge, and parent material) were referenced from the research of Hu et al. (2013).

Table 4
Pb and Sr isotopic ratios.

	Depth (cm)/Distance (m)	$^{87}Sr/^{86}Sr \pm 2\sigma$	Pb(mg/kg)	$^{206}Pb/^{207}Pb$	$^{208}Pb/(^{206}Pb + ^{207}Pb)$	$^{208}Pb/^{206}Pb$	$^{206}Pb/^{204}Pb \pm 2\sigma$	$^{207}Pb/^{204}Pb \pm 2\sigma$	$^{208}Pb/^{204}Pb \pm 2\sigma$
			Soil profiles total Pb contents and isotopic ratios						
p0	0–10	0.714178 ± 0.000012	53.40	1.1858	1.0993	2.0262	17.734 ± 0.005	14.954 ± 0.003	35.932 ± 0.006
p1	10–20	0.716339 ± 0.000012	44.20	1.1895	1.0952	2.0159	17.831 ± 0.008	14.990 ± 0.005	35.945 ± 0.009
p2	20–30	0.717503 ± 0.000009	38.40	1.1835	1.0996	2.0287	17.443 ± 0.004	14.738 ± 0.003	35.386 ± 0.008
p3	30–40	0.717569 ± 0.000008	40.40	1.1894	1.0985	2.0221	17.606 ± 0.008	14.802 ± 0.006	35.600 ± 0.009
p4	40–50	0.717935 ± 0.000011	43.00	1.1863	1.0997	2.0268	17.379 ± 0.008	14.650 ± 0.006	35.224 ± 0.010
p5	50–60	0.718179 ± 0.000010	45.30	1.1834	1.0976	2.0251	17.467 ± 0.007	14.760 ± 0.006	35.373 ± 0.009
p6	60–70	0.718265 ± 0.000009	44.10	1.1974	1.0873	1.9954	17.765 ± 0.003	14.837 ± 0.002	35.448 ± 0.004
p7	70–80	0.718362 ± 0.000009	45.00	1.1913	1.0981	2.0198	17.501 ± 0.006	14.691 ± 0.004	35.348 ± 0.008
p8	80–90	0.718490 ± 0.000013	45.20	1.1914	1.0932	2.0108	17.616 ± 0.005	14.786 ± 0.003	35.423 ± 0.006
p9	90–100	0.718482 ± 0.000011	42.90	1.1918	1.1032	2.0290	17.627 ± 0.003	14.791 ± 0.002	35.765 ± 0.005
b1	0	0.710165 ± 0.000011	76.40	1.1839	1.0968	2.0233	17.960 ± 0.006	15.170 ± 0.004	36.337 ± 0.008
b2	1	0.710547 ± 0.000012	73.80	1.1846	1.0985	2.0258	17.937 ± 0.006	15.142 ± 0.004	36.337 ± 0.010
b3	3	0.711612 ± 0.000015	56.70	1.1848	1.0984	2.0255	17.979 ± 0.005	15.175 ± 0.003	36.417 ± 0.008
b4	7	0.712534 ± 0.000016	41.10	1.1930	1.0945	2.0119	17.853 ± 0.007	14.966 ± 0.004	35.920 ± 0.009
b5	15	0.720851 ± 0.000014	41.20	1.2036	1.0963	2.0071	17.794 ± 0.005	14.784 ± 0.003	35.714 ± 0.010
b6	31	0.720935 ± 0.000012	39.90	1.2050	1.0981	2.0095	17.461 ± 0.006	14.491 ± 0.003	35.088 ± 0.009
b7	63	0.717609 ± 0.000016	36.90	1.2064	1.1050	2.0208	17.479 ± 0.003	14.489 ± 0.002	35.323 ± 0.004
b8	127	0.719260 ± 0.000015	40.50	1.2007	1.0976	2.0117	17.683 ± 0.007	14.728 ± 0.004	35.575 ± 0.008
b9	300	0.718709 ± 0.000011	42.90	1.2021	1.0934	2.0031	17.298 ± 0.004	14.391 ± 0.002	34.650 ± 0.007
			Soil profiles acid-extractable Pb contents and isotopic ratios						
p0	0–10		23.45	1.1737	1.1311	2.0947	17.301 ± 0.003	14.740 ± 0.003	36.240 ± 0.005
p1	10–20		17.25	1.1770	1.1281	2.0866	17.584 ± 0.004	14.940 ± 0.002	36.690 ± 0.006
p2	20–30		13.20	1.1775	1.1299	2.0896	18.310 ± 0.004	15.550 ± 0.003	38.260 ± 0.005
p3	30–40		12.50	1.1745	1.1388	2.1084	17.729 ± 0.007	15.095 ± 0.004	37.380 ± 0.008
p4	40–50		11.30	1.1789	1.1228	2.0752	17.579 ± 0.007	14.911 ± 0.008	36.480 ± 0.009
p5	50–60		13.60	1.1764	1.1367	2.1029	17.728 ± 0.005	15.070 ± 0.003	37.280 ± 0.007
p6	60–70		11.50	1.1821	1.1336	2.0925	18.370 ± 0.002	15.540 ± 0.002	38.440 ± 0.004
p7	70–80		30.75	1.1813	1.1326	2.0913	17.988 ± 0.002	15.227 ± 0.002	37.618 ± 0.005
p8	80–90		9.100	1.1817	1.1300	2.0862	17.347 ± 0.003	14.680 ± 0.003	36.190 ± 0.004
p9	90–100		9.800	1.1817	1.1280	2.0826	17.444 ± 0.003	14.762 ± 0.001	36.330 ± 0.003
b1	0		32.11	1.1655	1.1378	2.1142	17.572 ± 0.004	15.08 ± 0.003	37.150 ± 0.006
b2	1		28.85	1.1694	1.1469	2.1276	17.705 ± 0.006	15.14 ± 0.004	37.670 ± 0.009
b3	3		27.17	1.1772	1.1361	2.1012	17.847 ± 0.004	15.16 ± 0.003	37.500 ± 0.007
b4	7		11.58	1.1842	1.1354	2.0941	17.740 ± 0.006	14.980 ± 0.004	37.150 ± 0.008
b5	15		13.11	1.1841	1.1327	2.0892	17.748 ± 0.004	14.989 ± 0.003	37.080 ± 0.009
b6	31		18.50	1.1851	1.1450	2.1112	16.739 ± 0.004	14.124 ± 0.003	35.340 ± 0.007
b7	63		16.29	1.1854	1.1403	2.1023	16.739 ± 0.003	14.121 ± 0.001	35.190 ± 0.004
b8	127		16.16	1.1848	1.1418	2.1055	16.756 ± 0.005	14.142 ± 0.003	35.280 ± 0.006
b9	300		18.13	1.1833	1.1436	2.1100	16.698 ± 0.003	14.111 ± 0.002	35.232 ± 0.005

Source identification requires distinguishing between natural and anthropogenic Pb. Sturges and Barrie (1987) noted that anthropogenic sources of $^{206}Pb/^{207}Pb$ are relatively low, ranging from 0.96–1.20. The naturally occurring Pb was generally higher (> 1.20). As shown in Table 4, the total $^{206}Pb/^{207}Pb$ ratios were > 1.20, at > 31 m distance from the road, illustrating that the soil near the roadside (< 31 m) was influenced by anthropogenic sources, and far from the roadside (> 31 m) was not affected by anthropogenic sources. In the soil profile, the Pb isotope composition of the polluted soils was all < 1.20, illustrating that the anthropogenic pollution of Pb has been buried deep into the soil profile.

The $^{206}Pb/^{207}Pb$ ratios were much lower with acid-extractable Pb isotopic ratios than those with total digestion. This is indicative of anthropogenic Pb. As revealed by other researchers (Zhu et al., 2001; Li et al., 2011), the acid extraction, which can reflect the presence of an extraneous source of Pb in soil (Chen et al., 2007) was more sensitive than total digestion for detecting anthropogenic Pb. Therefore, acid-extractable Pb isotopic ratios were used to trace the sources in this paper. As shown in Fig. 4A and Fig. 4B), the good linear relationship between $^{206}Pb/^{204}Pb$ and $^{206}Pb/^{207}Pb$ illustrated that the Pb of soils may be described by the binary mixture model. In the profile (Fig. 4A), analysis indicated the binary mixing of two major Pb sources, which were parent material and vehicle exhaust (R^2 = 0.6903). In topsoil (Fig. 4B), at a distance of 0–7 m away from the roadside, the two sources were parent material and vehicle exhaust; however, at 31–300 m from the roadside, the sources were parent material and coal.

The anthropogenic Pb in soil samples can be estimated using the Eqs. (10) and (11) (Bird et al., 2010):

$$X_A = \frac{R_s - R_B}{R_A - R_B} \times 100\% \quad (10)$$

$$X_A + X_B = 100\% \quad (11)$$

where X_A, R_A, X_B, and R_B represent the contribution ratios and the isotopic ratios of Source A (parent material) and Source B (vehicle exhaust or coal), respectively. The results of contribution ratios were shown in Fig. 5. The calculated results were parent material at 73.66–81.77% (78.29% on average) and vehicle exhaust at 18.23–26.34% (21.71% on average), suggesting that parent material was the main source for Pb in the profile soils (Fig. 5A). Overall, with the increase of depth, contribution of parent material gradually increased. In the topsoil (Fig. 5B), parent material remained the main Pb source, the average value was 75.02%. The samples that were collected closer to the road (distance of 0-7 m) were influenced by vehicle exhaust. The contribution rates were 16.20% to 34.27% (24.04% on average), and with the increase of the distance, the contribution rates gradually decreased. Sites located far from the roadside (31–300 m), were mainly influenced by coal, with contribution rates from 24.94% to 28.31% (26.15% on average).

The results showed that at distances > 31 m away from the roadside, the impact of Pb on the soil was gradually weakened. Because the

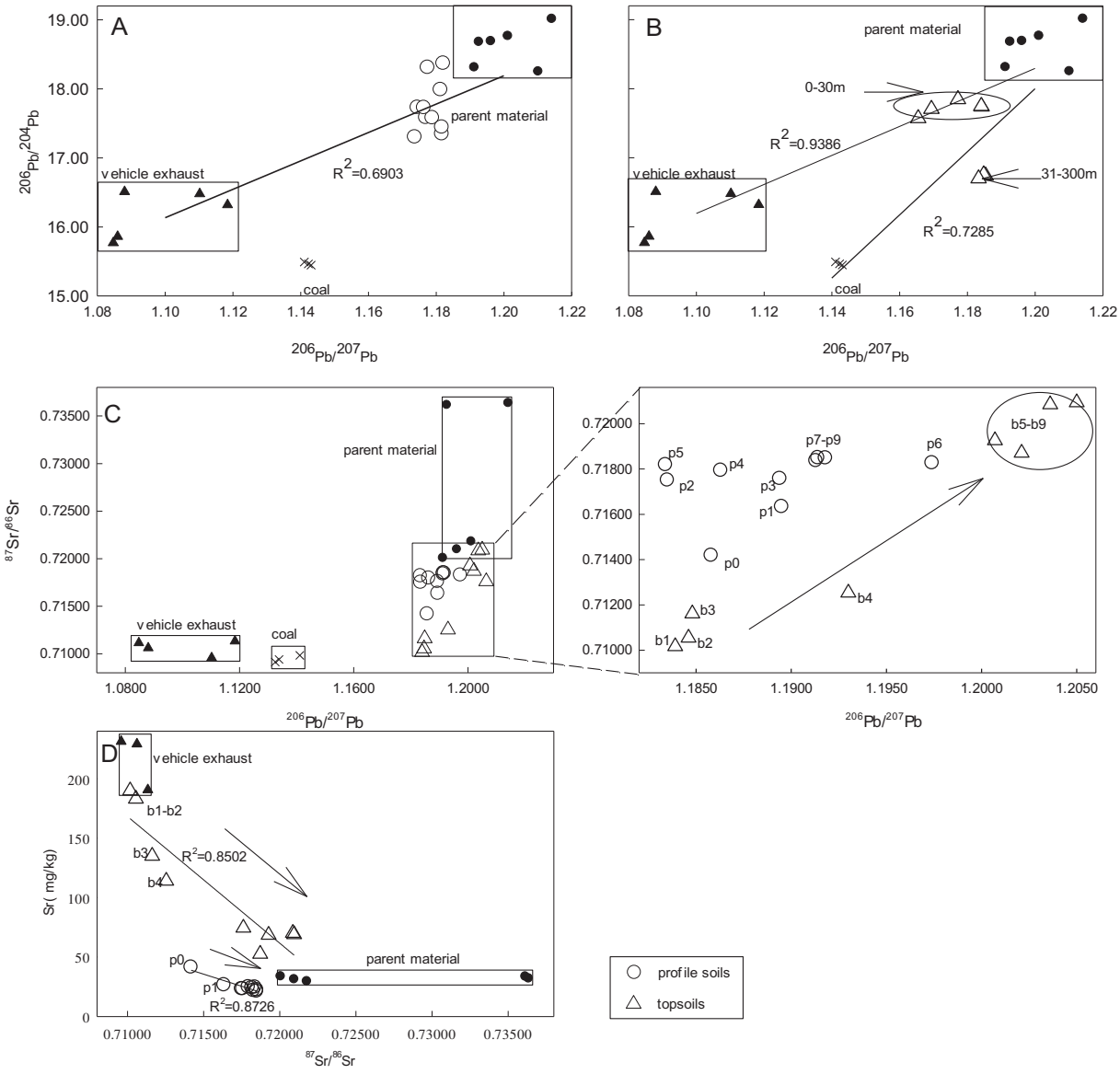

Fig. 4. Isotopic compositions in soils and potential sources. A: Acid-extractable $^{206}Pb/^{207}Pb$ radios versus $^{206}Pb/^{204}Pb$ of the profile soils and four possible end-members; B; Acid-extractable $^{206}Pb/^{207}Pb$ radios versus $^{206}Pb/^{204}Pb$ of the topsoils and four possible end-members; C: Catter plot of $^{206}Pb/^{207}Pb$ and $^{87}Sr/^{86}Sr$ ratios brings more constraints on the origin of soil; D: Relationship between $^{87}Sr/^{86}Sr$ and content of Sr.

location is distant from industrial areas, we suggest that it was mainly influenced by combustion of domestic coal. The influence on the soil profile gradually decreased with the increase of depth; the maximum value appears at the depth of 30–40 cm, which indicates that Pb pollution has a slight downward migration.

3.4.2. Strontium isotope tracing pollution sources

The isotopic compositions ($^{87}Sr/^{86}Sr$) of the soils were shown in Table 4. The changes in $^{87}Sr/^{86}Sr$ and Sr concentrations (Table 1) were reversed, with larger values of $^{87}Sr/^{86}Sr$ occurring with lower Sr concentrations, and smaller influences from anthropogenic pollution sources (Widory et al., 2010). Relationship between $^{87}Sr/^{86}Sr$ and content of Sr were shown in Fig. 4D. For profile soils, a significant relationship can be observed by using linear regression ($R^2 = 0.8726$, $p < 0.01$), which suggested that Sr was controlled by mixing sources of vehicle exhaust and parent material. The direction of arrow indicates that the more $^{87}Sr/^{86}Sr$ with the more of the depth of the profile, and the anthropogenic pollution is less obvious. For the topsoils, the direction of arrow show that, the farther away from the road, the less obvious anthropogenic contamination. The samples within 7 m(b1-b4) away from the road are distributed in the vehicle exhaust.

3.4.3. Combined Pb-Sr isotope tracing pollution sources

Combining the two-isotope system ($^{206}Pb/^{207}Pb$ and $^{87}Sr/^{86}Sr$) generates even more constraints on the source of soil sources. Samples with anthropogenic sources had lower $^{87}Sr/^{86}Sr$ values (Widory et al., 2010). Profile soils had high $^{87}Sr/^{86}Sr$ (0.714178–0.718490) and high $^{206}Pb/^{207}Pb$ (1.1834–1.1974), mainly affected by parent material (Fig. 4C). As Fig. 4C showed, samples of topsoil from the road 0-7 m(b1-b4) are affected by vehicle exhaust or coal but this contribution reduced as the distance increased to 31 m, primarily replaced by the influence of parent material. Similarly, for the profile, with the increase depth, the soils gradually close to the parent material, the influence of topsoil is mainly affected by anthropogenic sources. The results are consistent with that of Pb and Sr isotopes.

4. Conclusions

The metal contents in the studied roadside soil were mainly distributed in the 0–7 m closest to the road, and within the 30–200 m from

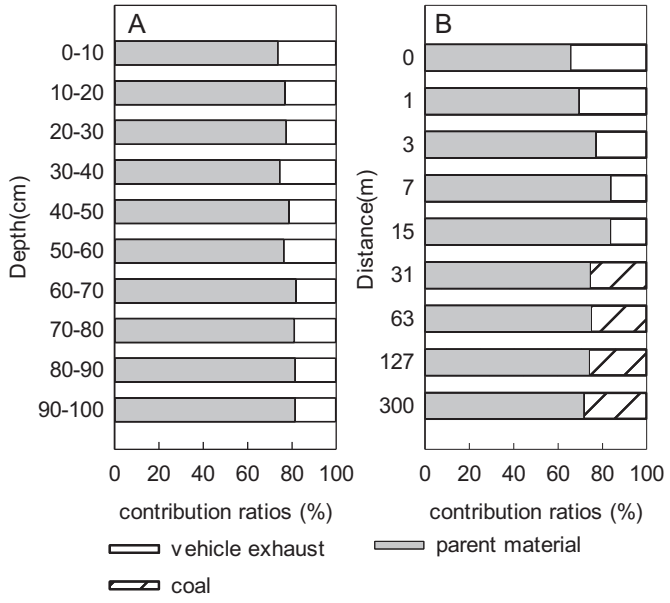

Fig. 5. Percentage contribution of main sources to acid-extractable Pb of soil; A, profile soil; B, topsoil.

the road, they reached the background values for soil. In vertical profiles, Cu, Zn, Rb, Sr, Cd, In, Ba and Pb showed clear aggregation. The results of the EFs, E_r indexes of the profile indicated that most soils were classified as uncontaminated slightly contaminated. The Cd values showed the highest E_r. The E_r of Pb and Zn should also not be ignored. Therefore, the main metal pollution factors in soil along the road were Cd, Zn and Pb, which were the main pollutant of traffic pollution indicated by the EPA (U·S Environmental Protection Agency). According to the human health risk assessment, there is no risk for human health in the roadside.

According to multivariate statistical analysis, soil was clearly affected by the traffic factors and also by the industrial production.

The Pb isotopic tracing results of the study demonstrate that sources of Pb mainly originated from parent material (78.29%) and vehicle exhaust (21.71%) in the profile, and with the increase of depth, the contribution of parent material slightly increased. The samples that were collected closer to the road (distance of 0–7 m) were influenced by vehicle exhaust. The contribution rates were 24.04% on average, and with the increase of the distance, the contribution rates decreased gradually. Sites located at a greater distance from the road (31–300 m), were influenced by coal, with contribution rates from 24.94% to 28.31% (26.15% on average). The Sr isotopic tracing results of the study demonstrate that the sources of Sr in profile originated from parent material, and the samples of topsoil from the road 0–7 m are also affected by vehicle exhaust. Combining the Pb and Sr isotopes confirmed that the main sources of the soil are parent material and also affected by vehicle exhaust and coal.

Acknowledgement(s)

This work was supported by the National Science Foundation of China (21177043, 21377042), the Natural Science Foundation of Fujian Province (2016J01065, 2015J01147), State Key Laboratory of Environmental Geochemistry (SKLEG2016901) and Science and technology project of Quanzhou (2014Z130). The authors express heartfelt thanks to the colleagues who participated in the sampling work. Thanks to anonymous reviewers and their constructive comments.

References

Adamo, P., Giordano, S., Sforza, A., Bargagli, R., 2011. Implementation of airborne trace element monitoring with devitalised transplants of *Hypnum cupressiforme* Hedw.: assessment of temporal trends and element contribution by vehicular traffic in Naples city. Environ. Pollut. 159, 1620–1628.

Ali, Z., Malik, R., Shinwari, Z., Qadir, A., 2015. Enrichment, risk assessment, and statistical apportionment of metals in tannery-affected areas. Int. J. Environ. Sci. Technol. 12, 537–550.

Azeez, J.O., Mesele, S.A., Sarumi, B.O., et al., 2014. Soil metal pollution as a function of traffic density and distance from road in emerging cities: a case study of Abeokuta, southwestern Nigeria. Arch. Agron. Soil Sci. 60, 275–295.

Bird, G., Brewer, P.A., Macklin, M.G., Nikolova, M., Kotsev, T., Mollov, M., Swain, C., 2010. Quantifying sediment-associated metal dispersal using Pb isotopes: application of binary and multivariate mixing models at the catchment-scale. Environ. Pollut. 158, 2158–2169.

Carrero, J.A., Goienaga, N., Olivares, M., et al., 2012. Raman spectroscopy assisted with XRF and chemical simulation to assess the synergic impacts of guardrails and traffic pollutants on urban soils. J. Raman Spectrosc. 43, 1498–1503.

Carrero, J.A., Arrizabalaga, I., Bustamante, J., et al., 2013. Diagnosing the traffic impact on roadside soils through a multianalytical data analysis of the concentration profiles of traffic-related elements. Sci. Total Environ. 458–460, 427–434.

Chan, D., Stachowiak, G., 2004. Review of automotive brake friction materials. Proc. Inst. Mech. Eng. D. 218, 953–966.

Chang, J., Liu, M., Li, X.H., et al., 2009. Primary research on health risk assessment of metals in road dust of Shanghai. China Environ. Sci. 29, 548–554 (In Chinese).

Chen, C.X., Zhuang, Z.X., Liu, H.B., 2007. Source differentiation by lead isotope ratios in total digests of soil fractions and residual fractions. Chin. J. Anal. Chem. 35, 103–105.

Chen, D.Y., Xie, W.B., Song, G., et al., 2010a. Heavy metal pollution and potential ecological risk of paddy field soil in littoral area, Fujian province. Chin. J.f Soil Sci. (in Chinese). 41, 194–199.

Cheng, H.F., Hu, Y.A., 2010. Lead isotopic fingerprinting and its applications in lead pollution studies in China: a review. Environ. Pollut. 158, 1134–1146.

Chen, X., Xia, X., H, Zhao Y, Zhang P., 2010b. Heavy metal concentrations in roadside soils and correlation with urban traffic in Beijing, China. J. Hazard. Mater. 181, 640–646.

Dantu, S., 2009. Metals concentration in soils of southeastern part of Ranga Reddy district, Andhra Pradesh, India. Environ. Monit. Assess. 149, 213–222.

Dao, L., Morrison, L., Zhang, C., 2010. Spatial variation of urban soil geochemistry in a roadside sports ground in Galway, Ireland. Sci. Total Environ. 408, 1076–1084.

Dong, P., Xiao, R.G., 2005. Caesium application and caesium (alkali metals) resource evaluation. China Min. Mag. 14, 30–34 (in Chinese).

Fang, Wen-wen, Li, Zhang, Ye, Sheng-xia, et al., 2015. Pollution evaluation and health risk assessment of metals from atmospheric deposition in Anqing. China Environ. Sci. 35, 3795–3803 (in Chinese).

Ferreira-Baptista, L., De Miguelb, E., 2005. Geochemistry and risk assessment of street dust in Luanda, Angola: a tropical urban environment. Atmos. Environ. 39, 4501–4512.

Fujiwara, F., Rebagliati, R.J., Marrero, J., et al., 2011. Antimony as a traffic-related element in size-fractionated road dust samples collected in Buenos Aires. Microchem. J. 97, 62–67.

Gunawardena, J., Abdul, M., Ziyath, P.E., et al., 2015. Sources and transport pathways of common metals to urban road surfaces. Ecol. Eng. 77, 98–102.

Gunawardena, J., Ziyath, A.M., Egodawatta, P., et al., 2014. Influence of traffic characteristics on polycyclic aromatic hydrocarbon build-up on urban road surfaces. Int. J. Environ. Sci. Technol. 11, 2329–2336.

Hakanson, L., 1980. An ecological risk index for aquatic pollution control, a sedimentological approach. Water Res. 14, 975–1001.

Harrison, R.M., Tilling, R.B., Romero, M.S., Harrad, S., Jarvis, K., 2003. A study of trace metals and polycyclic aromatic hydrocarbons in the roadside environment. Atmos. Environ. 37, 2391–2402.

Hedberg, E., Gidhagen, L., Johansson, C., 2005. Source contributions to PM10 and arsenic concentrations in Central Chile using positive matrix factorization. Atmos. Environ. 39, 549–561.

Hu, G.R., Yu, R.L., Zheng, Z.M., 2013. Application of stable lead isotopes in tracing heavy-metal pollution sources in the sediments. J. Environ. Sci. 33, 1326–1331.

Jang, H.N., Seo, Y.C., Lee, J.H., et al., 2007. Formation of fine particles enriched by V and Ni from heavy oil combustion: anthropogenic sources and drop-tube furnace experiments. Atmos. Environ. 41, 1053–1063.

Kadi, M.W., 2009. Soil pollution hazardous to environment: a case study on the chemical composition and correlation to automobile traffic of the roadside soil of Jeddah city, Saudi Arabia. J. Hazard. Mater. 168, 1280–1283.

Kayhanian, M., 2012. Trend and concentrations of legacy lead (Pb) in highway runoff. Environ. Pollut. 160, 169–177.

Klaminder, J., Farmer, J.G., Mackenzie, A.B., 2011. The origin of lead in the organic horizon of tundra soils: atmospheric deposition, plant translocation from the mineral soil or soil mineral mixing. Sci. Total Environ. 409, 4344–4350.

Kumar, M., Furumai, H., Kurisu, F., Kasuga, I., 2013. Tracing source and distribution of metals in road dust, soil and soakaway sediment through speciation and isotopic fingerprinting. Geoderma 211-212, 8–17.

Lee, C.S., Li, X., Shi, W., et al., 2006. Metal contamination in urban, suburban, and country park soils of Hong Kong: a study based on GIS and multivariate statistics. Sci. Total Environ. 356, 45–61.

Li, H.B., Yu, S., Li, G.L., et al., 2011. Contamination and source differentiation of Pb in the park soils along an urban–rural gradient in Shanghai. Environ. Pollut. 159, 3536–3544.

Li, W.H., Tian, Y.Z., Shi, G.L., et al., 2012. Concentrations and sources of PAHs in surface sediments of the Fenhe reservoir and watershed, China. Ecotoxicol. Environ. Saf. 75, 198–206.

Li, X., Feng, L., 2012. Multivariate and geostatistical analyzes of metals in urban soil of Weinan industrial areas, Northwest of China. Atmos. Environ. 47, 58–65.
Li, Z.Y., Ma, Z.W., Kuijp, T.J., et al., 2014. A review of soil heavy metal pollution from mines in China: pollution and health risk assessment. Sci. Total Environ. 468–469, 843–853.
Man, Y.B., Sun, X.L., Zhao, Y.G., et al., 2010. Health risk assessment of abandoned agricultural soils based on heavy metal contents in Hong Kong, the world's most populated city. Environ. Int. 36, 570–576.
Martinez, J., Llamas, J.F., Miguel, E., et al., 2008. Soil contamination from urban and industrial activity: example of the mining district of Linares southern Spain. Environ. Geol. 54, 669–677.
Mazzei, F., D'Alessandro, A., Lucarelli, F., et al., 2008. Characterization of particulate matter sources in an urban environment. Sci. Total Environ. 401, 8–19.
Meza-Montenegro, M.M., Gandolfi, A.J., Santana-Alcántar, M.E., et al., 2012. Metals in residential soils and cumulative risk assessment in Yaqui andMayo agricultural valleys, northern Mexico. Sci. Total Environ. 433, 472–481.
Morton-Bermea, O., Hernández-Álvarez, E., González-Hernández, G., et al., 2009. Assessment of heavy metal pollution in urban topsoils from the metropolitan area of Mexico City. J. Geochem. Explor. 101, 218–224.
Nardi, L.V.S., Formoso, M.L.L., Müller, I.F., et al., 2013. Zircon/rock partition coefficients of REEs, Y, Th, U, Nb, and ta in granitic rocks: uses for provenance and mineral exploration purposes. Chem. Geol. 335, 1–7.
Negrel, P., Petelet-Giraud, E., 2012. Isotopic evidence of lead sources in Loire River sediment. Appl. Geochem. 27, 2019–2030.
Oliva, S.R., Espinosa, A.J.F., 2007. Monitoring of metals in topsoils, atmospheric particles and plant leaves to identify possible contamination sources. Microchem. J. 186, 131–139.
Qian, P., Zheng, X.M., Zhou, L.M., et al., 2011. Magnetic properties as indicator of heavy metal contaminations in roadside soil and dust along G312 highways. Procedia Environ Sci 10 (Part B), 1370–1375.
Querol, X., Viana, M., Alastuey, A., et al., 2007. Source origin of trace elements in PM from regional background, urban and industrial sites of Spain. Atmos. Environ. 41, 7219–7231.
Rajsi, C.S., Miji, C.Z., Tasi, C.M., et al., 2008. Evaluation of the levels and sources of trace elements in urban particulate matter. Environ. Chem. Lett. 6, 95–100.
Šajn, R., Gosar, M., 2014. Multivariate statistical approach to identify metal sources in Litija area Slovenia. J. Geochem. Explor. 138, 8–21.
Sawyer, R.F., Harley, R.A., Cadle, S.H., et al., 2000. Mobile sources critical review: 1998 NARSTO assessment. Atmos. Environ. 34, 2161–2181.
Sindern, S., Lima, R.F.S., Schwarzbauer, J., et al., 2007. Anthropogenic heavy metal signatures for the fast-growing urban area of Natal NE-Brazil. Environ. Geol. 52, 731–737.
Sturges, W.T., Barrie, L.A., 1987. Lead 206/207 isotope ratios in the atmosphere of North America as tracers of US and Canadian emissions. Nature 329, 144–146.
Sun, G.X., Wang, X.J., Hu, Q.H., 2011. Using stable lead isotopes to trace heavy metal contamination sources in sediments of Xiangjiang and Lishui Rivers in China. Environ. Pollut. 159, 3406–3410.
Sun, J.W., Hu, G.R., Yu, R.L., et al., 2016. Tracing sources of heavy metals in the soil profiles of drylands by multivariate statistical analysis and lead isotope[J]. Environ. Sci. 37, 2304–2312 (in Chinese).
Thorpe, A., Harrison, R.M., 2008. Sources and properties of non-exhaust particulate matter from road traffic: a review. Sci. Total Environ. 400, 270–282.
Townsend, A.T., Seen, A.J., 2012. Historical lead isotope record of a sediment core from the Derwent River Tasmania, Australia: a multiple source environment. Sci. Total Environ. 424, 153–161.
Turekian, K.K., Wedepohl, K.H., 1961. Distribution of the elements in some major units of the earth's crust. Geol. Soc. Am. Bull. 72, 175–192.
U.S. DOE, 2004. RAIS: Risk assessment information system [EB/OL]. http://risk.lsd.ornl.gov/raphp.shtml.
U.S. Environmental Protection Agency, 1989. Risk Assessment Guidance for Superfund, Vol. I: Human Health Evaluation Manual[EB/OL]. http://www.epa.gov/superfund/programs/risk/ragsa/index.htm.
U.S. Environmental Protection Agency, 2009. Risk Assessment Guidance for Superfund, vol. I: Human Health Evaluation Manual Part F, Supplemental Guidance for Inhalation Risk Assessment. http://www.epa.gov/superfund/programs/risk/ragsa/index.htm.
U.S. Environmental Protection Agency, 1996. Soil Screening Guidance: Technical Background Document. (1996-5). http://www.epa.gov/superfund/resources/soil/toc.htm#p1.
U.S. Environmental Protection Agency, 2001. Supplemental Guidance for Developing Soil Screening Levels for Super Fund Sites[EB/OL]. (2001-03-27). http://www.epa.gov/superfund/health/conmedia/soil/pdfs/ssgmarch01.pdf.
Wang, Z., Liu, S.Q., Chen, X.M., et al., 2008. Estimates of the exposed dermal surface area of Chinese in view of human health risk assessment. J. Saf. Environ. 8, 152–156 (in Chinese).
Werkenthin, M., Kluge, B., Wessolek, G., 2014. Metals in European roadside soils and soil solution - a review. Environ. Pollut. 189, 98–110.
Wawer, M., Magiera, T., Ojha, G., et al., 2015. Characteristics of current roadside pollution using test-monitoring plots. Sci. Total Environ. 505, 795–804.
Widory, D., Liu, X., Dong, S., 2010. Isotopes as tracers of sources of lead and strontium in aerosols TSP & PM2.5 in Beijing. Atmos. Environ. 44, 3679–3687.
Wu, S., Peng, S.Q., Zhang, X.X., et al., 2015. Levels and health risk assessments of metals in urban soils in Dongguan, China. J. Geochem. Explor. 148, 71–78.
Wu, Y.G., Xu, Y.N., Zhang, J.H., et al., 2010. Evaluation of ecological risk and primary empirical research on metals in polluted soil over Xiaoqinling gold mining region, Shaanxi, China. Trans. Nonferrous Metals Soc. China 20, 688–694.
Wysocka, I., Vassileva, E., 2016. Determination of cadmium, copper, mercury, lead and zinc mass fractions in marine sediment by isotope dilution inductively coupled plasma mass spectrometry applied as a reference method. Microchem. J. 128, 198–207.
Yang, Z.F., Wang, Y., Shen, Z.Y., et al., 2009. Distribution and speciation of metals in sediments from the mainstream, tributaries, and lakes of the Yangtze River catchment of Wuhan, China. J. Hazard. Mater. 166, 1186–1194.
Ye, C., Li, S., Zhang, Y., Zhang, Q., 2011. Assessing soil heavy metal pollution in the water-level-fluctuation zone of the Three Gorges Reservoir, China. J. Hazard. Mater. 191, 366–372.
Zhang, M.M., Lu, X.W., Chen, H., et al., 2015. Multi-element characterization and source identification of trace metal in road dust from an industrial city in semi-humid area of Northwest China. J. Radioanal. Nucl. Chem. 303, 637–646.
Zhao, Y., Yu, R.L., Hu, G.R., et al., 2017. Chemical characteristics and Pb isotopic compositions of PM2.5 in Nanchang, China. Particuology 32, 95–102.
Zhu, B.Q., Chen, Y.W., Peng, J.H., 2001. Lead isotope geochemistry of the urban environment in the Pearl River Delta. Appl. Geochem. 16, 409–417.